

Angular Dependence of the Neutron-Induced Fission Process. II*

J. E. BROLLEY, JR., W. C. DICKINSON,† AND R. L. HENKEL
Los Alamos Scientific Laboratory, University of California, Los Alamos, New Mexico

(Received February 14, 1955)

The angular anisotropy of neutron-induced fission has been studied with a double fission chamber. For U^{235} at 7.4 Mev and Np^{237} at 14.3 Mev, the variation of the differential fission cross section was found to depend strongly on the fourth power of the cosine of the angle between the fission fragment and the neutron beam. For U^{235} a resonance-type dependence of the anisotropy on neutron energy has been observed. Qualitative indication that the light and heavy fission fragment groups have slightly different anisotropies has been obtained in the case of Np^{237} at 14.3 Mev.

INTRODUCTION

IN previous work¹ it has been shown that the fragments of fission induced by 14-Mev neutrons were anisotropically distributed in the center-of-mass system. This property was observed in varying degree for five different nuclei. The data were represented approximately by angular distributions of the form $(1 + A \cos^2\theta)$. To expand knowledge of this phase of fission mechanics, the present experiments have been directed to additional questions. How does the anisotropy change with the bombarding neutron energy? Do the light and heavy fragments participate equally in the process? What is the more precise form of the angular distribution? To these ends we have extended the earlier work through the use of an improved coincidence apparatus.

A theory giving information on these questions does not exist in the present literature. The collective model of Hill and Wheeler² and the shell-structure model of Fong³ are recent theories which may be adapted to the interpretation of these phenomena.

EXPERIMENTAL METHODS

The early studies¹ were performed with a simple parallel-plate ionization chamber. The present experiments have utilized a collimated double fission chamber which is described in detail in the next section. In addition to providing fission rates at various angles with respect to the neutron beam it supplies the ionization spectra of the two groups of fission fragments at these angles. It also provides data for the precise study of ionization spectra from thermal neutron fission. (See Fig. 5.) The light-fragment group which has the highest energy is clearly differentiated from the heavy-fragment group by a deep valley. As the energy of the fission-inducing neutrons increases, the valley in the ionization spectrum becomes more shallow. This has been shown

by Wahl⁴ in ionization chamber studies at 2.5 and 14 Mev. Moreover, radiochemical studies⁵ indicate a rapid increase in the probability of symmetric fission with rising neutron energy. Thus the distinction between the light and heavy groups tends to vanish as the fission inducing particle gives more energy to the reaction.

At 14-Mev neutron energy, however, the two groups are still readily identified despite the rise in the valley. At this energy one has the possibility of discerning relative changes in the angular distributions of the light and heavy groups. If the effect is marked, it would manifest itself by an increase in area of one group and decrease in area of the other in the ionization spectrum of the fragments. The angular variation of the fission cross section is given by the integral over both groups of the spectrum measured at various angles.

APPARATUS

Fission Chamber

The fission chamber described in reference 1 had several properties susceptible of improvement. Fission fragments lost a considerable fraction of their energy in traversing the long collimator passages so that the energy distribution could not be observed. Also, background pulses attributed to alpha particle pile-up, $n-p$ and $n-\alpha$ reactions, and to recoiling atoms of the chamber gas were of the same magnitude as those pulses from the lowest-energy fission fragments. These effects required small but uncertain corrections to be made to the data.

To minimize these effects a collimated double fission chamber was constructed. A cross section of this chamber is shown schematically in Fig. 1. A common negative high-voltage electrode serves a Frisch grid chamber and a simple parallel-plate "coincidence" chamber. This electrode is 0.066 inch thick and honeycombed with 0.016-inch diameter holes over a one-inch diameter area to serve as a collimator for the fission fragments. The optical transmission of the collimator is 59 percent. Only coincident fission pulses in the two chambers are

* This document is based on work performed under the auspices of the U. S. Atomic Energy Commission.

† Present address: University of Indonesia, Bosscha Laboratory, Bandung, Java, Indonesia.

¹ W. C. Dickinson and J. E. Brolley, Jr., *Phys. Rev.* **90**, 388 (1953); J. E. Brolley, Jr. and W. C. Dickinson, *Phys. Rev.* **94**, 640 (1954).

² D. L. Hill and J. A. Wheeler, *Phys. Rev.* **89**, 1102 (1953).

³ Peter Fong, *Phys. Rev.* **89**, 332 (1953), and privately circulated manuscript.

⁴ J. S. Wahl, *Phys. Rev.* **95**, 126 (1954).

⁵ R. W. Spence and G. P. Ford, *Ann. Revs. Nuclear Sci.* **2**, 399 (1953).

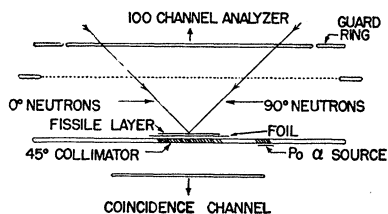


FIG. 1. Schematic cross section of double fission chamber.

counted. To attain complete symmetry between the 0° and 90° angular settings, the collimator holes are inclined at 45° to the electrode normal. The extreme angular resolution of the collimator is $9\frac{3}{4}^\circ$ and the most probable angle of emission with respect to the collimator axis is 4° . This is poorer resolution than was employed in the first chamber but was necessary to increase the fission counting rates and to keep to a minimum the energy loss in the collimator passages of fragments entering the coincidence chamber. A foil, thin to fission fragments, upon which is evaporated a layer of fissile material, is mounted directly over the collimator area on the Frisch grid side. Whereas those fragments entering the coincidence chamber must pass through the foil and collimator passages before expending their residual energy in the chamber, the fragments entering the Frisch grid chamber lose negligible energy in the fissile layer, providing it is kept very thin. Hence an accurate fission ionization spectrum can be obtained. An identical honeycombed area, $\frac{1}{4}$ inch in diameter, adjacent to the main collimator serves to collimate Po alpha particles entering the Frisch grid chamber. These particles are emitted from a monomolecular Po film deposited electrochemically on a silver backing which is attached to the collimator plate. They are used to help calibrate the pulse-energy scale and test the equipment.

A copper-gasketed steel purifier filled with calcium chips continuously purified the chamber gas mixture (argon + CO_2). The purifier was initially outgassed for 24 hours at 200°C . With gas in the chamber the purifier was maintained at 150°C . At this temperature O_2 and H_2O contaminants were removed but the CO_2 fraction was not significantly affected.

Electronics

A block diagram of the electronic circuitry is shown in Fig. 2. Associated with every fission signal in the coincidence chamber, there is a signal produced in the Frisch grid chamber. These coincident pulses were amplified by preamplifiers with cathode follower outputs mounted directly behind the chamber and completely shielded by a cylindrical metal shell. The temperature of the preamplifiers was held constant to within one degree centigrade by a thermostatically controlled heater. After traversing RG 71/U cable to the control room, the pulse from the Frisch grid chamber, went to a Model 250 gated linear amplifier which

also provided proper delay. The amplified pulse from the coincidence chamber was applied to a modified Harwell discriminator and pulse shaper having the desirable feature of generating a square wave output pulse only after the input pulse, if greater than the threshold setting, has reached its peak value. Thus the time delay of the output pulse was not a function of the amplitude of the input pulse as in the case with conventional discriminators. The output of the Harwell circuit created a 3-microsecond gate in the Model 250 amplifier, arriving about 0.2 microsecond before the pulse from the Frisch grid chamber. Output pulses from the amplifier, after an additional amplification by a window amplifier, inserted to gain distribution resolution, were analyzed by a Wilkinson type 100-channel pulse-height analyzer.⁶

For calibration, a Model 500 pulse generator was connected to feed artificial pulses to both preamplifiers so that the analyzer output could be calibrated directly in terms of millivolt input to the Frisch grid pre-amplifier.

Pulses in the coincidence chamber channel could be suitably delayed for the determination of the accidental coincidence rate.

Chamber Tests

In the design of the Frisch grid side of the fission chamber the paper of Bunemann, Cranshaw, and Harvey⁷ was followed. The grid served to shield the collecting electrode from charges induced by the electrons and positive ions in the region of the chamber traversed by the fission fragments. The output pulse induced by the electrons moving from the grid region to the collector was closely proportional to the original number of ion pairs produced. Unfortunately, the requirement that there be no electron collection by the grid made it impossible to obtain complete shielding of the collector.

Following the notation of Bunemann *et al.*, the important parameters of our chamber are: radius of kovar

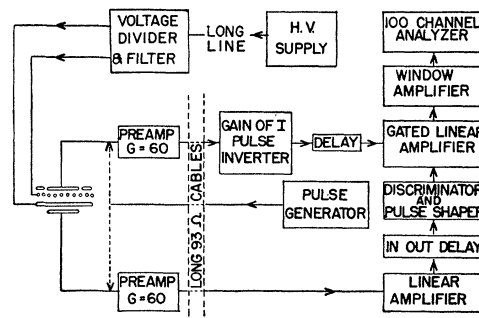


FIG. 2. Block diagram of electronics.

⁶ Hiebert, Evans, and Watts, Los Alamos Scientific Laboratory Report LA-1565, April, 1953 (unpublished).

⁷ Bunemann, Cranshaw, and Harvey, Can. J. Research A27, 191 (1949).

grid wires, $r=6.35 \times 10^{-3}$ cm, grid wire spacing $d=0.107$ cm, source-grid distance $a=2.60$ cm, grid-collector distance $p=1.21$ cm, $\rho=0.373$, $l=0.0174$. The inefficiency of shielding $\sigma=l/(p+l)=1.4$ percent. The minimum ratio of grid-collector to source-grid voltage to insure zero grid interception was calculated to be 1.03, corresponding to a ratio of the fields equal to 2.22.

Tests were made with monoenergetic alpha particles to compare the theoretical analysis of reference 7 with actual performance. For this work both uncollimated U^{234} and U^{235} alpha particles from a 10-microgram/cm² evaporated layer of uranium oxide and collimated Po α particles were used. An argon+5 percent CO₂ gas mixture was used at a total pressure of 900 mm Hg. This was sufficient to stop all alpha particles before reaching the grid region.

Results of measuring the pulse height of the U^{234} and Po alpha groups for different values of R , the ratio of grid-collector to source-grid voltage, are shown in Fig. 3. The theory is well confirmed since there is a noticeable increase in pulse height when R is increased from 1.0 to 1.1 but negligible difference when a further increase to 1.2 is made in R . A value of R equal to 1.1 was used in subsequent work.

The "supersaturation" effect, characteristic of argon + CO₂ mixtures, is observed in Fig. 3. This decrease in pulse height as the collecting voltage is increased beyond a certain point has been variously attributed to electron capture resonances in gas impurities, inelastic collisions between electrons and CO₂ molecules when the electron drift velocity reaches a certain threshold, and resonant reactions with the CO₂ molecules resulting in a break-up of the molecule and to electron attachment to one of the components. Despite this disadvantage it was

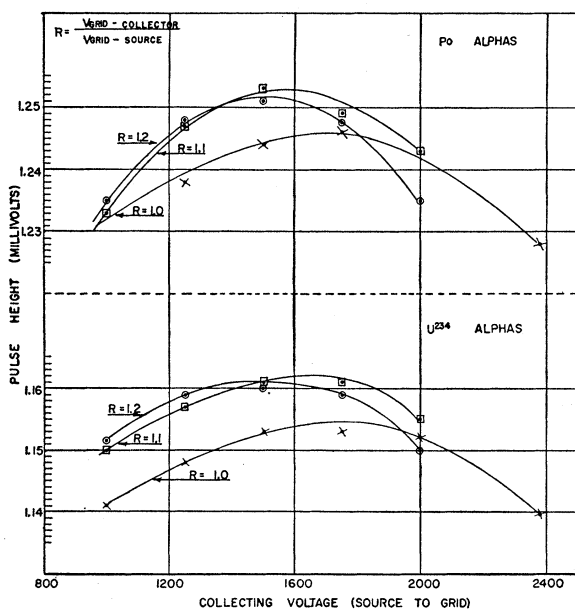


FIG. 3. Pulse height of Po and U^{234} α particles as a function of collecting voltage for different values of R .

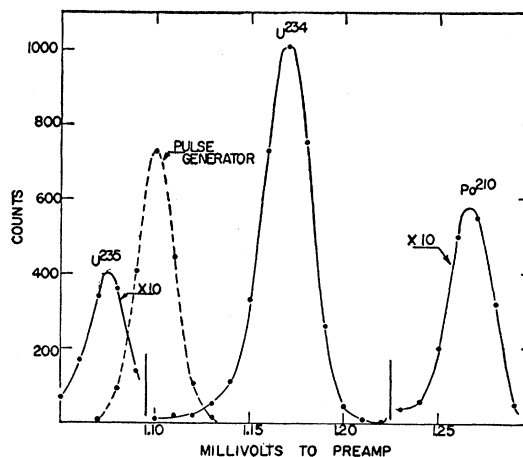


FIG. 4. Typical α pulse-height distribution. $R=1.1$ total chamber voltage, 3000.

found that the high electron drift velocity, low saturation voltage, and lack of hydrogen content made argon + CO₂ mixtures preferable for these experiments.⁸

A typical alpha pulse-height spectrum is shown in Fig. 4. The small low energy tail on the U^{234} peak is attributed to alpha particles traveling at grazing angles to the source foil. The total widths at half-maximum of the uncollimated U^{234} and collimated Po peaks are 2.56 percent and 2.22 percent respectively. The corresponding width of the pulse generator distribution is 2.14 percent. An rms subtraction of this electronic noise contribution to the widths results in "chamber" widths of 1.41 percent and 0.60 percent, respectively. It is assumed that the contribution of the pulse generator to the electronic width is negligible. The lack of 100 percent shielding efficiency and the dependence upon alpha particle trajectory of the amount of charge induced on the collector by positive ions causes the spread to be greater for the uncollimated alphas.

As a test of the over-all operation of the equipment the thermal fission spectra of U^{233} and U^{235} were observed.⁹ The U^{233} and U^{235} foils were in the form of a 15- μ g/cm² painted layer of U^{233} and a 10- μ g/cm² evaporated layer of U^{235} respectively. The two spectra are shown in Fig. 5.

The ionization produced by a fission fragment was converted to an energy scale by comparison with the ionization produced by alpha particles. The energy obtained in this way for the most probable light and heavy fragments is called the ionization energy. This differs from the true energy because the last few Mev of the fragment energy are lost in nonionizing processes.¹⁰ The difference between the true energy and the ionization energy is termed the ionization defect. Leachman¹¹

⁸ W. N. English and G. C. Hanna, Can. J. Phys. **31**, 768 (1953).

⁹ Neutrons were obtained from the thermal column of the Los Alamos Water Boiler.

¹⁰ Knipp, Leachman, and Ling, Phys. Rev. **80**, 478 (1950).

¹¹ R. B. Leachman, Phys. Rev. **87**, 444 (1952).

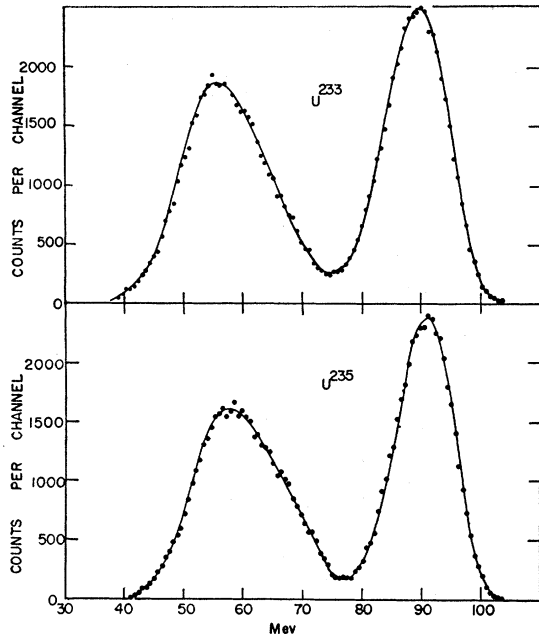


FIG. 5. U^{233} and U^{235} thermal fission spectra.

has estimated that the ionization defects in argon gas are about 5.7 and 6.7 Mev for the most probable light and heavy fragments respectively.

To compare the present values for the most probable energies of the light and heavy fragments with those obtained in the careful work of Brunton and Hanna¹² who used an argon+3 percent CO_2 mixture, it was necessary to know how the ionization defect varies with the gas mixture. Recently, ionization defect differences have been measured for a variety of gases¹³ including pure argon and argon+3 percent CO_2 . It was found that the defects in the mixture were 3.0 and 4.5 Mev greater than those in pure argon for the most probable light and heavy fragments respectively. If one assumes that this difference depends linearly on the percentage of CO_2 then the defects for argon+5 percent CO_2 would be 2 and 3 Mev greater than those for argon+3 percent CO_2 , for the most probable light and heavy fragments respectively. To compare the measured energy values with those of Brunton and Hanna (see Table I) these energy increments have been added. Also the values have been corrected by 0.2 and 0.1 Mev respectively for fragment mean energy loss in the U^{233} and U^{235} layers. The values listed for Brunton and Hanna were corrected for source and collimator losses. The agreement would appear to be satisfactory except perhaps in the case of the heavy fragment of U^{233} where the measured value is 4.4 percent higher than those of Brunton and Hanna.

¹² D. C. Brunton and G. C. Hanna, Can. J. Research **A28**, 190 (1950).

¹³ Lloyd O. Herwig and Glenn H. Miller, Phys. Rev. **95**, 413 (1954).

14-Mev Neutron Source

The source of 14-Mev neutrons was the $T(d,n)He^4$ reaction, using the atomic beam of 250-kev deuterons from the Los Alamos Cockcroft-Walton accelerator. The beam was magnetically analyzed and collimated before striking a zirconium-tritium target. The neutron flux was monitored by counting a known fraction of the alpha particles generated in the $d+T$ reaction. The error in relative neutron monitoring for various runs was about 1 percent. The active foil of the coincidence chamber was 10 cm from the target.

Data were collected in a series of symmetric, repeated runs so as to minimize the effects due to electronic drifts and deterioration of the neutron source. Since the source to foil spacing was so close, no correction was made for the small scattered-neutron backgrounds.

Other Energies

The neutron sources for the other energies were the $T(p,n)He^3$, $D(d,n)He^3$, and $T(d,n)He^4$ reactions. Protons or deuterons were accelerated by the large Los Alamos Van de Graaff generator and were precisely

TABLE I. Most probable fission-fragment ionization energies.

	Fragment	Brunton and Hanna	Present work
U^{233}	Light	93.0	92.0
	Heavy	56.6	59.1
U^{235}	Light	94.5	93.0
	Heavy	60.2	61.1

magnetically analyzed and controlled. The experimental area was some 20 feet from the earth so that the room-scattered and thermal-neutron background was negligible. The target assembly consisted of a thin-walled gas chamber 10 cm long and 1 cm in diameter and had either a 1/20 mil nickel entrance foil or a 1/2-mil molybdenum entrance foil. Target pressures of deuterium and tritium of 1 to 2 atmospheres and beam intensities up to 10 μa were used to obtain large enough neutron intensities for collecting data in a reasonable time. The fission chamber was located in the forward direction with respect to the accelerated beam to intercept the highest neutron flux. The position was adjusted as close to the target as the rotation of the chamber would permit. Neutron intensities were monitored by both a long counter and by integration of the beam current. No correction was made for background neutrons caused by room scattering or internal scattering in the apparatus. Background measurements made for previous experiments in similar geometry indicated that such corrections would be small. The effects of neutrons produced in the target foil, etc., were measured by replacing the target gas by hydrogen or vacuum.

The errors introduced by these extraneous neutrons were negligible.

EXPERIMENTAL RESULTS

Uranium-235

The first set of data were obtained using an evaporated layer of $U^{235}O_2$, 0.5 mg/cm², on a gold backing 0.9 mg/cm². Irradiations with neutrons of various energies were performed at the large Los Alamos Van de Graaff Generator. In this study we have sought to ascertain the energy dependence of the anisotropic distribution of fragments by measuring the quantity $\sigma_f(0^\circ, E_n)/\sigma_f(90^\circ, E_n)$ at a number of different neutron energies. The results are compiled in Table II and graphically exhibited in Fig. 6. Data for thermal and 14-Mev neutrons are from the earlier work.¹ The energy limits indicated for E_n represent the extreme neutron energy spread intercepted by the fissile layer resulting from degradation of the accelerated charged particles in the gas target and by geometrical factors. The standard deviations indicated represent a combination of statistical errors and allowances for systematic errors. Accidental coincidences occurring during these meas-

TABLE II. $0^\circ/90^\circ$ anisotropy in U^{235} fission as a function of neutron energy.

E_n (Mev)	0	2.5	4.6	7.5 ^a	14.3	20.4
$0^\circ/90^\circ$ Intensity ratio	0.99 ±0.05	1.02 ±0.05	1.13 ±0.06	1.36 ±0.05	1.27 ±0.08	1.11 ±0.09

^a Average of measurements at 7.4 and 7.6 Mev.

urements were inconsequential. The standard deviations of the angular settings probably did not exceed two degrees. Where necessary, small corrections were made to the zero-degree data to take into account the effect of the finite angular resolution of the apparatus. Recent measurements with the $T(d,n)He^4$ reaction show that additional low-energy neutrons are produced in the source when the high-energy neutrons are greater than about 20 Mev. These measurements allow an approximate calculation of the yield of these low-energy neutrons under the experimental conditions at the time the 20.4-Mev ratio was determined. The error introduced to the ratio by these neutrons is probably small compared to the error indicated in Fig. 6.

We also observed the variation of the relative differential fission cross section at 7.4 Mev with the same fissile layer. This was done to provide a more accurate expansion of the differential fission cross section in even powers of cosine θ than was possible with the earlier data. Figure 7 portrays the result in the center-of-mass system together with a least squares fitted expansion of the form $1 + A \cos^2\theta + B \cos^4\theta$. For the goodness of fit S^2 , we assign the value 1.6×10^{-3} . It is clear that the fourth power of the cosine is dominant; a fact not

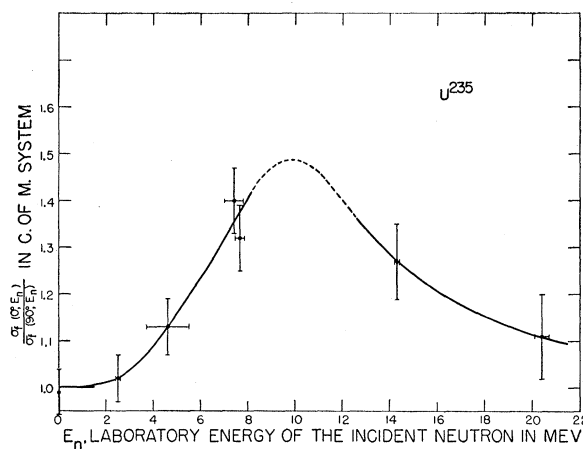


FIG. 6. Energy dependence of the anisotropy.

evident in our earlier data. The least squares fit yields $\sigma_f(0^\circ, 7.4)/\sigma_f(90^\circ, 7.4) = 1.36$ in harmony with our preceding survey.

Neptunium-237

After completion of the U^{235} experiments a Np^{237} fissile layer was installed in the ionization chamber. This source was prepared by evaporating a deposit of $Np^{237}O_2$ to a thickness of about 60 $\mu\text{g}/\text{cm}^2$ on a 1.1-mg/cm² nickel foil. Irradiation of the neptunium was performed at the Los Alamos Cockcroft-Walton machine with 14.3-Mev neutrons.

The first phase of this study was the study of the fission fragment ionization spectrum at 0° (backwards) and 90° . Data were accumulated by taking many short runs at each angle until the integral count was 5000 at each position. Electronic drifts were negligible, hence the various runs were simply added. The summed data as presented by the 100-channel analyzer at 0° are illustrated in Fig. 8. The low-energy background can be removed by a short extrapolation of the spectrum into the abscissa. This correction is small and contributes a negligible error. From these measurements we

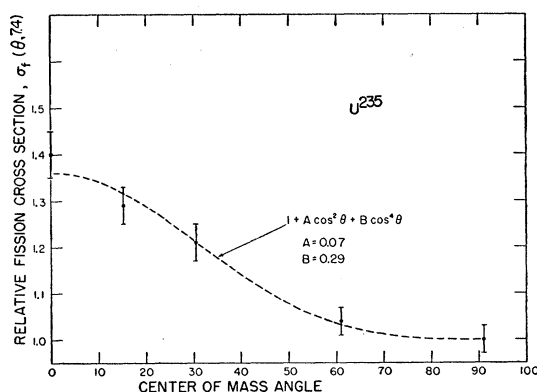


FIG. 7. Relative differential fission cross section of U^{235} at $E_n = 7.4$ Mev.

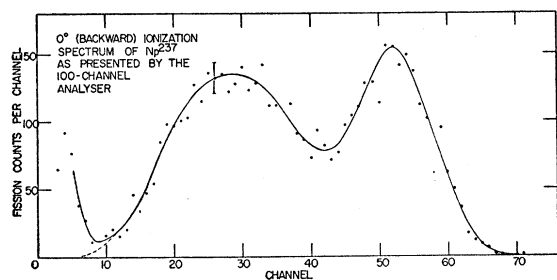


FIG. 8. Example of raw data presented by the 100-channel analyzer.

obtain $\sigma_f(0^\circ, 14)/\sigma_f(90^\circ, 14) = 1.16 \pm 2$ percent (c.m.). This may be compared with our previous value of 1.15 obtained in (1). In Fig. 9 the smoothed data of both positions are illustrated. The 0° (backward) curve is shifted toward lower energy because of center-of-mass motion. In order to compare the shapes more clearly, both curves were reduced to equal areas and their centroids were approximately superimposed in Fig. 10. This pattern will symmetrically invert about 90° (neglecting small center-of-mass effects); hence one sees that the heavy group tends to go forward with a somewhat higher probability than the light group. For reasons previously mentioned it is difficult to make a quantitative estimate of this effect. One may obtain a measure which is principally of qualitative significance by arbitrarily assuming that the minimum between the two groups separates them. This assumption is not strictly valid. On this premise one finds that there are about 10 percent more light fragments at 180° than at 90° . Or, inversely, at 0° there are about 10 percent more heavy fragments than at 90° , for the same total number of fissions at each angle. From the known kinetics of 14-Mev neutron-induced fission in U^{235} , one infers that center-of-mass motion can have only a relatively small influence on this phenomenon in Np^{237} . It seems probable therefore that this is a real effect in the center-of-mass system. The qualitative character, it must be re-emphasized, should be clearly borne in

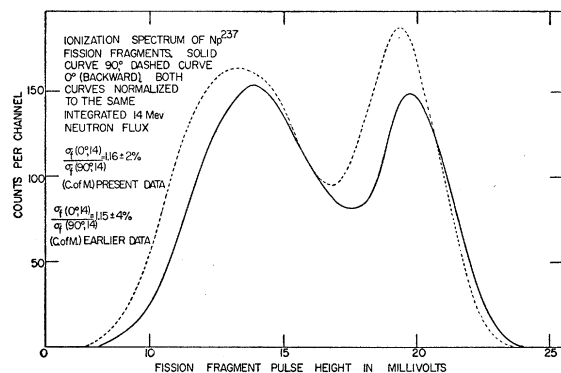


FIG. 9. Smoothed fission-fragment ionization spectra at 0° and 90° .

mind. We anticipate performing more certain experiments of this nature in the future.

In the second phase of the neptunium experiments, relative differential fission cross sections at 0° , 30° , 60° , and 90° in the laboratory system were measured. Accumulation of data proceeded by short runs at chosen angles until each angle had approximately 2000 counts. As in the case of U^{235} this was an attempt to obtain a representation of the fission cross section in even powers of $\cos\theta$. The 15° point was not obtained, but as in the uranium data, one sees by inspection of Fig. 11 that the fission cross section depends principally on the fourth power of the cosine. This least squares fitted distribution is assigned a goodness of fit $S^2 = 4 \times 10^{-4}$. The fitted curve yields $\sigma_f(0^\circ, 14)/\sigma_f(90^\circ, 14)$

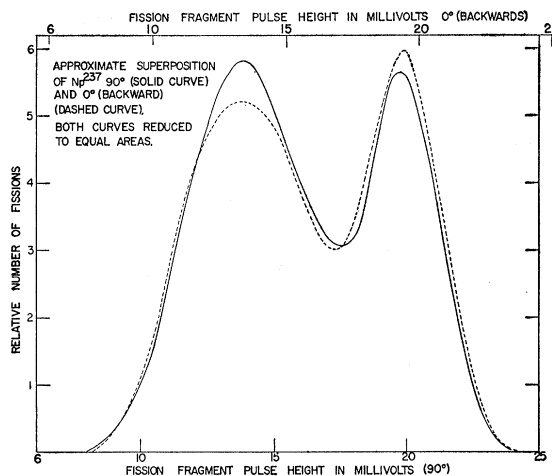


FIG. 10. Superposition of 0° and 90° ionization spectra after reduction to equal areas.

$= 1.18$ (c.m.) in good agreement with the other measurements on neptunium.

DISCUSSION

In this work, three properties of the anisotropic variation of the fission cross section were established; two being rather well founded, and one tentative. In both U^{235} and Np^{237} , at certain energies, the angular variation of the fission cross section exhibits a strong dependence on the fourth power of the cosine. The interpretation of this result is not clear but it would be instructive to compare the coefficients in both cases with the quadrupole moments of the two nuclei. This could afford insight as to how the process depended on the shape of the nucleus. Only two nuclei have been studied and therefore such conclusions may not be of a very general nature. We therefore plan to extend these studies to other fissionable nuclei.

The resonance character of energy dependence of the anisotropy seems moderately well established, though additional data are desirable, on U^{235} as well as other

nuclei. The decline of the anisotropy may well be associated with the rapidly increasing probability of symmetric fission with neutron energy.

The preponderance of heavy fragments in the forward direction likewise is susceptible of improved observation. Thus this experiment could be performed with U^{238} at 2.5-Mev neutron energy. In this region it is known that the ratio of the height of the higher-energy peak to valley minimum in the ionization spectrum is at least 3.3 whereas in the case of Np^{237} it was only about 2.

The progress of this experiment was possible only through the assistance of many of our associates. In particular we thank L. K. Schlacks for evaporating the fissile layers, R. W. Davis for untiring help in setting up the apparatus at the Cockcroft Walton machine and operating the accelerator, Group P-4 for the generous allotment of time on this accelerator, R. K. Zeigler

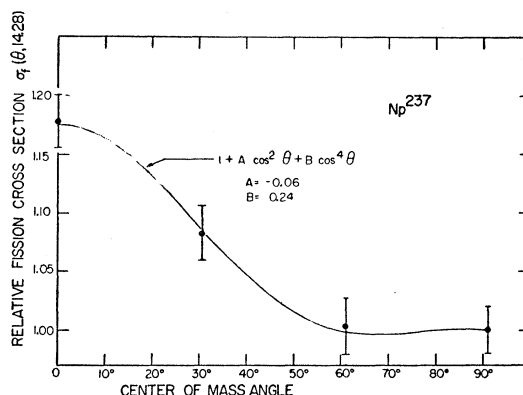


FIG. 11. Relative differential fission cross section of Np^{237} at $E_n = 14.3$ Mev.

for computational aid, and J. Waugh for graphical assistance.

Isobaric Triplet $Cr^{48} - V^{48} - Ti^{48*}\dagger\dagger$

RAYMOND K. SHELINE AND JOSEPH R. WILKINSON

Department of Chemistry, Florida State University, Tallahassee, Florida

(Received February 28, 1955)

Cr^{48} has been produced by the nuclear reaction $Ti^{46}(\alpha, 2n)Cr^{48}$. The gamma spectra of this nuclide have been investigated and peaks found at 118 kev and 307 kev. The two gamma rays are in coincidence and have the same intensity. The gamma rays of the daughter nuclide V^{48} have been shown to appear in the gamma spectra as Cr^{48} decays. The half-life of Cr^{48} has been determined as 24 ± 1 hours. The energy of the Cr^{48} orbital electron capture has been shown to be approximately 1.30 Mev with a very low ft value. A decay scheme for the isobaric triplet $Cr^{48} - V^{48} - Ti^{48}$ is proposed. Using the proposed decay schemes as a basis, the masses of Cr^{48} and V^{48} have been calculated to be 47.96934 ± 22 and 47.96749 ± 7 , respectively.

INTRODUCTION

CHROMIUM-48 has been reported as an orbital electron capturing activity produced in the spallation of iron with 340-Mev protons.¹ Its half-life was reported to be 23 or 24 hours. No gamma radiations were reported for this nuclide. Cr^{48} is an even-even nucleus with an associated $0+$ ground state² whereas V^{48} , the product nucleus, is known to have a ground state of $4+$ or $5+$.³ The decay of Cr^{48} may therefore be expected to be complex with the emission of gamma rays.

* This work was supported in part by the U. S. Atomic Energy Commission.

† This paper is taken from a portion of a thesis submitted by J. R. Wilkinson to the Graduate Faculty of Florida State University in partial fulfillment of the requirements for the Ph. D. degree.

‡ A paper on the decay of Cr^{48} was presented before the New York Meeting of the American Physical Society, 1955 [van Lieshout, Greenberg, and Wu, *Bull. Am. Phys. Soc.* **30**, No. 1, 32 (1955)].

¹ Rudstam, Stevenson, and Folger, *Phys. Rev.* **87**, 358 (1952).

² M. G. Mayer, *Phys. Rev.* **78**, 16 (1950).

³ Casson, Goodman, and Krohn, *Phys. Rev.* **92**, 1517 (1953).

This work was undertaken in an effort to produce Cr^{48} and to study its decay scheme and the decay scheme of its daughter V^{48} . Because of the great number of radionuclides produced in a spallation reaction, it was decided to attempt to produce Cr^{48} by alpha bombardment of titanium. The nuclear reaction expected was $Ti^{46}(\alpha, 2n)Cr^{48}$. The bombardment of enriched Ti^{46} was indicated since normal titanium contains only 8 percent Ti^{46} .

EXPERIMENTAL

Enriched Ti^{46} as TiO_2 was bombarded by 50-Mev alpha particles in the 60-inch cyclotron at the University of California for a period of 4 hours. The total beam current for the bombardment was 12.4 microampere hours.

The TiO_2 together with 10 mg of chromium as Cr_2O_3 and 10 mg of vanadium as V_2O_5 was fused with anhydrous sodium carbonate for a period of 30 minutes. The melt was extracted with hot water and filtered. A few drops of 6*N* NaOH was added to the filtrate